Journal of
Composites Science

MDPI

Article

Technical Feasibility of a Thermally Activated Nanotape for Electromagnetic Interference Applications

Kaiyu Cai [1], Dan Zhang [2] and Jose M. Castro [2,*]

[1] Key Laboratory for Organic Electronics & Information Displays (KLOEID), Institute of Advanced Materials (IAM) and School of Materials Science and Engineering, Nanjing University of Posts and Telecommunications, 9 Wenyuan Road, Nanjing 210046, China; cai.533@buckeyemail.osu.edu
[2] Integrated Systems Engineering, The Ohio State University, Columbus, OH 43210, USA; dan.zhang517@gmail.com
* Correspondence: castro.38@osu.edu

Abstract: Multiwalled carbon nanotube (MWCNT) nanopaper (NP)-reinforced in-mold coating (IMC) nanocomposites were fabricated by dip soaking without organic solvent. The thermally activated IMC resin was selected to provide electromagnetic interference shielding protection for sheet molding compound (SMC) material as well as other plastic materials due to the proven good adhesion of IMC resin to the substrate. In this work, the technical feasibility of a continuous fabrication process was evaluated for a nanopaper/IMC (NP/IMC) composite. The curing behavior of the candidate IMC resin was studied for a better understanding of the fabrication of NP/IMC nanotape as a prepreg (with 10% polymerization), as well as the final curing once the nanotape was applied to the substrate. The required limiting maximum temperature to prevent curing during infiltration was established. This allows the fabrication of multilayer nanotape or coatings by stacking several layers of tape to improve the EMI shielding protection. To be specific, the average EMI shielding effectiveness for a one-layer composite was 21 dB, while it increased to 48 dB on average for a six-layer composite.

Keywords: EMI shielding; multiwalled carbon nanotube nanopaper; in-mold coating resin; process window

Citation: Cai, K.; Zhang, D.; Castro, J.M. Technical Feasibility of a Thermally Activated Nanotape for Electromagnetic Interference Applications. *J. Compos. Sci.* **2023**, *7*, 325. https://doi.org/10.3390/jcs7080325

Academic Editor: Francesco Tornabene

Received: 10 July 2023
Revised: 29 July 2023
Accepted: 2 August 2023
Published: 8 August 2023

1. Introduction

Electromagnetic interference (EMI) resulting from electronic devices with high packing density contains numerous unwanted radiated signals, which may result in the intolerable degradation of communication systems or severe damage to the safety of electronic devices [1,2], and could even cause health hazards [3,4]. This pollution has even become crucial in recent years due to the application of more immense power and higher frequencies of electromagnetic waves [5].

To attenuate the interference, electrically conducting materials, such as metals and conductive polymer composites, are usually utilitzed to reflect or absorb the incident electromagnetic waves [6]. EMI shielding by absorption nowadays, however, is more important for many applications than EMI shielding by reflection [6]. Although metals or materials with a metallic coating exhibit very high EMI shielding effectiveness (EMI SE) (up to 100 dB), their intrinsic drawbacks limit their application in many scenarios; i.e., metals are high-density, easily corroded, and low absorbents of electromagnetic waves [5,6]. These drawbacks may result in the rusty bolt effect of nonlinearity causing intermodulation issues, thus affecting the overall performance and reliability of equipment or systems, especially operating in sea environments [2]. Thus, conductive polymer composites are usually suggested for these applications [7,8]. Moreover, some researchers also apply ferromagnetic iron oxide (Fe_3O_4) as its synergetic effect with CNT allows a broader effective absorption range and stronger absorption at microwave frequencies [9,10].

To provide polymer composites with enough conductivity, carbon-based nanoparticles have been used in various polymer matrices as electrical reinforcements for their low percolation threshold [11–13]; i.e., a tiny amount of these materials can provide sufficient electrical conductivity. Previous results suggest that polymers filled with high-aspect-ratio nanofillers usually possess high EMI SE (multiwalled carbon nanotubes > carbon nanofiber > carbon black) [14,15]. However, unsuitable dispersion methods could significantly decrease the EMI SE and increase the required percolation threshold value, thus increasing the cost of composites [13,16]. However, it is not easy to obtain a uniform dispersion of carbon nanotubes (CNTs) in a polymer resin, especially for a high concentration (usually > 5 wt.%), due to their large saurface area (~1500 m^2/g) [11,17,18], which significantly increases the viscosity of resins. A bad dispersion of CNTs may also result in the aggregation of CNTs and, thus, decrease the mechanical properties of composites [11].

To solve this issue, CNTs can be dispersed in water or an organic solvent, after which the dispersion can be filtered under a vacuum to prepare a paper-like thin film, often called CNT nanopaper (CNT NP) [11]. Resins then can be infiltrated into the CNT NP substrate to prepare CNT NP/polymer composites [11].

Previous researchers have found that the selection of the polymer matrix does not significantly affect the EMI SE, especially the absorption and reflection of waves [11–14]. Thus, the selection of a polymeric matrix is mainly based on the envisioned applications. To obtain well-infiltrated CNT NP/polymer composites, resins should have a viscosity of less than 1 Pa·s at a low shear rate (e.g., 1 s^{-1}) [19,20]. The commercial in-mold coating (IMC) resin developed by OMNOVA Solutions Inc. (now Synthomer) has already been demonstrated to have good adhesion to sheet molding compound (SMC) material, PC, PC/ABS, and TPO [21]. Thus, CNT NP/IMC composites have great potential to be used as commercial products, and their acceptance by industry should be easier due to the commercial success of the IMC process.

Herein, we used MWCNT NP and IMC resin to prepare an MWCNT NP/IMC composite. In this study, we evaluated the technical feasibility of the process. The curing behavior was characterized for a better understanding of the fabrication of NP/IMC nanotape (with 10% polymerization) and the full curing as coatings. EMI shielding protection was also analyzed to better understand the NP/IMC composite.

2. Experimental

2.1. Materials

In this work, the MWCNTs were purchased from Hengqiu Graphene Technology Co., Ltd. (Suzhou, China) with a diameter of 8–15 nm, a length of 3–12 μm, and a purity of >95 wt.%. The surfactant used to disperse the CNT in water, sodium dodecyl sulfate (SDS), was purchased from Sigma-Aldrich (St. Louis, MO, USA).

The resin in the composite is a one-component heat-activated resin supplied by Synthomer (previously OMNOVA Solutions Inc., Beachwood, OH, USA) with a density of 1.258 g/cm^3 and a viscosity of 4.5 to 8.2 Pa·s at 30 °C. The initiator used in this research is T-butyl peroxybenzoate (TBPB, Akzo Nobel, Richmond, CA, USA). A typical composition of the resin is shown in Table 1 [22].

Table 1. Components of a single-component IMC [22].

Component	Weight (%)
LP90 (polyvinyl acetate in styrene)	20.00
Urethane 783 (unsaturated urethane oligomers)	20.00
Chemlink 600 (polyoxyethylene glycol dimetharrylate)	10.00
Hydroxypropyl methacrylate	10.00
Styrene	15.00
2% benzoquinone	1.70

Table 1. *Cont.*

Component	Weight (%)
t-Butyl peroxybenzoate	1.00
Zinc stearate	2.00
12% cobalt octoate	0.10
Talc	20.20

2.2. Sample Preparation

The preparation of the MWCNT NP is detailed in references [11,12]. In brief, an MWCNT was first dispersed in water containing the surfactant SDS. The mixture was then sonicated for 4 h, after which the NP was prepared by pouring the solution through a PTFE membrane (TriSep Corporation, Goleta, CA, USA) utilizing vacuum filtration. The NP was ready for use after 24 h of drying in an oven. The SEM image shown in Figure 1 [12] confirms the effective dispersion of nanotubes with 30–100 nm pores. A pilot-scale continuous manufacturing process of the nanopaper was developed based on this method, as shown in Figure 2 [12]. All the water and surfactant used to disperse MWCNTs can be recycled; thus, no waste is generated by the manufacturing process. The nanostructured MWNT NP has a very low permeability [12], and thus for an industrially viable process, it is desired to provide a preimpregnated nanopaper or nanotape, which serves as the final coating.

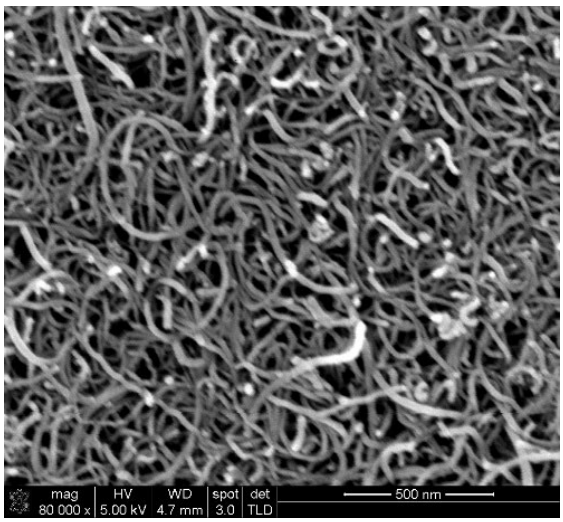

Figure 1. SEM image of MWCNT nanopaper.

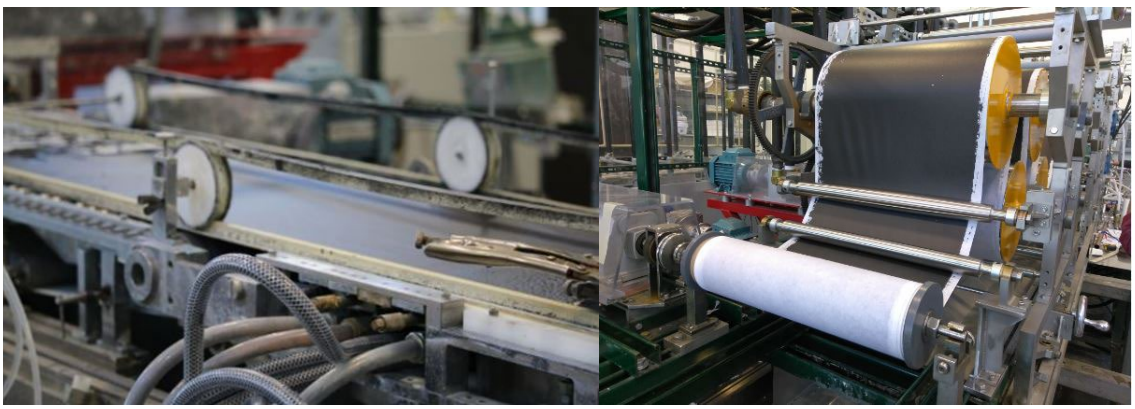

Figure 2. A continuous nanopaper fabrication process on a pilot scale.

For the resin infiltration, the heat-activated resin was first degassed and mixed with 1.75 wt.% of TBPB at 50 °C for 10 min (200 rpm). After degassing, the NP was infused with the resin by dip soaking at 50 °C for another 10 min.

2.3. Characterization

2.3.1. Rheology

Viscosity measurements were carried out with a TA ARES-G2 rheometer using a 25 mm parallel plate with a 1 mm gap. Temperature sweep viscosity tests were carried out between 30 and 100 °C with a shear rate of 1 s^{-1}. The rheology result of IMC resin is shown in Figure 3. It can be seen that the viscosity did not change much after 50 °C.

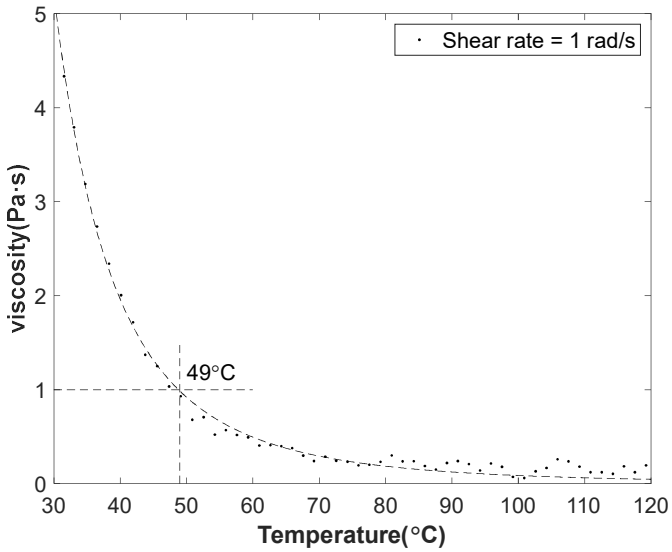

Figure 3. Temperature sweep viscosity test for IMC resin with a shear rate of 1 rad/s.

2.3.2. Thermal Gravimetric Analysis (TGA)

The weight percentage of the nanocomposites was measured on a TGA 550 instrument from 30 °C to 800 °C in a nitrogen environment (flow rate: 40 mL/min) as carried out in our previous work [11,12].

2.3.3. SEM

The fracture surface microstructure morphology of the NP/IMC nanocomposites (from a tensile test) was observed under a Carl Zeiss Ultra 55 plus field-emission SEM. The samples were sputter-coated before SEM characterization. Both low-resolution and high-resolution images were taken.

2.3.4. Cure Model

As the main chemical reaction of the IMC involves the vinyl groups, cure models were developed to describe the curing process for IMC resin in three steps, i.e., initiation, propagation, and termination. The detailed cure models can be found in [21]. However, as the initial concentration of the inhibitor and initiator were kept fixed in this work, the inhibition time can be determined using a simplified free radical model, while the propagation process can be expressed by an autocatalytic model with an assumed initial conversion of 0.001 at $t = t_z$ [22]. The simplified model is represented by Equations (1) and (2), as shown below [21–23].

$$t_z = e^{\left(\frac{E_d}{RT} - k_d\right)} \quad (1)$$

where t_z is the inhibition time in seconds, E_d is the reaction constant, R is the ideal gas constant, T is the temperature in K, and k_d is the frequency constant.

$$\frac{d\alpha}{dt} = k_p \alpha^m (\alpha_{max} - \alpha)^n, where\ k_p = k_{p0} e^{-\frac{E_P}{RT}} \quad (2)$$

where k_p is the kinetic rate constant, E_p is the activation energy, k_{p0} is the pre-exponential factor, m and n are reaction orders, and α_{max} is the maximum conversion, which is a temperature-related variable.

2.3.5. Differential Scanning Calorimetry (DSC) Tests

The parameters for the cure model were obtained via DSC tests with a TA Q20 differential scanning calorimeter in a nitrogen atmosphere. The typical temperature for IMC curing utilized in industry is over 130 °C, while DSC experiments need to be performed at temperatures no higher than 120 °C, because there is always a lag time before the recording of DSC devices. Although the temperature at which predictions are needed is out of the experimental range, previous researchers have demonstrated the reliability of this method by comparing the predictions with experimental results [22–24].

Polymerization at low temperatures is usually not complete. In order to investigate this issue, a dynamic DSC scan is usually conducted after the isothermal scan to evaluate the residual cure after the isothermal run. The maximum dynamic scan temperature is typically 250 °C to assure 100 percent conversion [22]. The degree of cure, a time-related variable, can be calculated with the following equation. The maximum conversion can also be calculated with this equation.

$$\alpha(t) = \frac{1}{H_{total}} \int_0^t \left(\frac{dH}{dt} \right) dt \quad (3)$$

where H is the heat, t is time, and H_{total} is the total heat for complete conversion.

In this work, DSC experiments were conducted at 90 °C, 100 °C, 110 °C, and 120 °C to generate curing curves and, thus, cure models, as shown in Figure 4.

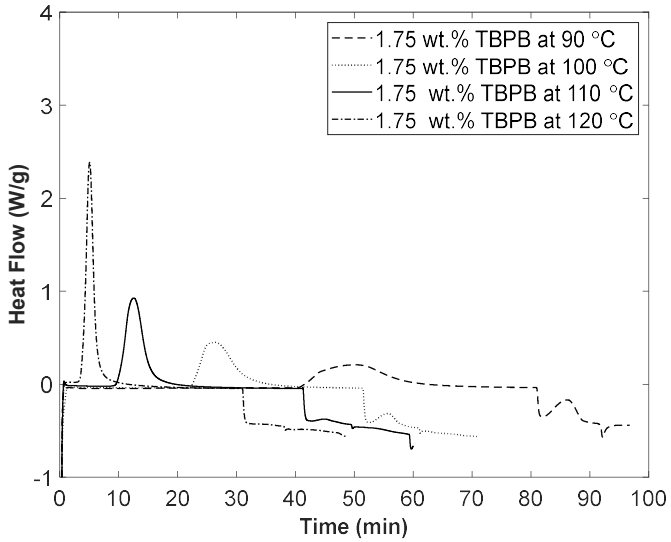

Figure 4. DSC curves for uncured NP/IMC composite at 90, 100, 110, and 120 °C.

2.3.6. EMI Shielding Test

The electromagnetic shielding effectiveness (EMI SE) of the nanopaper composites was tested under ASTM standard D4935 using an N5230A PNA-L network analyzer (Agilent Technologies, Santa Clara, CA, USA) ranging from 13 MHz to 1.5 GHz, which typically belongs to the very high frequency (VHF) and ultra high frequency (UHF) of the radio

wave range. The set-up consisted of a sample holder (two 6-inch-diameter brass halves) with an input and output connected to the network analyzer [11,12].

3. Results and Discussion

3.1. Process Window Study for NP/IMC Composite

A process window is used to delimitate the suitable controllable process parameters for the fabrication of NP/IMC composites.

For good infiltration, because the viscosity of resins is required to be less than 1 Pa·s [25], the infiltration temperature for IMC resin (with 1.75 wt.% initiator) should be higher than 50 °C, as shown in Figure 3. For the upper limit of the infiltration temperature, the infiltration temperature should also be no higher than 80 °C to avoid any polymerization in the infiltration step for a typical soaking time of 10 min, as can be deduced from Figure 4. Thus, a suitable temperature range for the infiltration of IMC resin is 50–80 °C. However, for a continuous process, the recommended temperature for the infiltration is 50 °C (also used in this work) to make sure that no reaction occurs during the infiltration process. Moreover, lower infiltration temperatures are also favorable for process control and economics.

TGA and SEM tests were conducted for the fully cured NP/IMC composite (cured at 150 °C for 12 h). The quantitative analysis of TGA suggests that the CNT weight percentage of the composite was around 28 wt.%, which is similar to the result of our previous NP/polymer composites [11,12] and thus indicates the feasibility of this process. For the qualitative analysis of microstructure morphology, both the low- and high-resolution images of NP/IMC composite show that the pores of the NP were filled by IMC resin, as shown in Figure 5. No voids being observed also confirms the feasibility of this process.

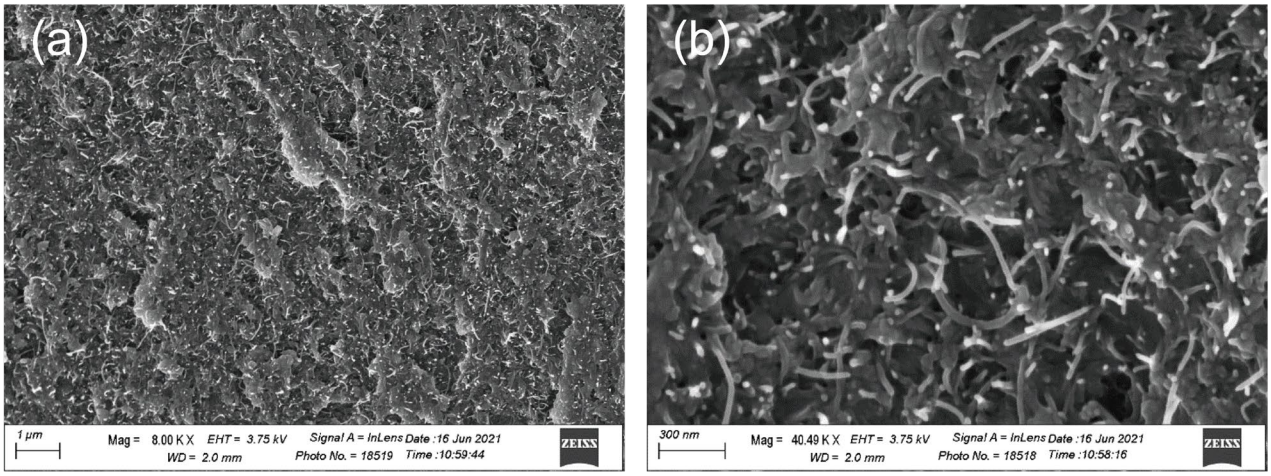

Figure 5. SEM images of fully cured NP/IMC composite under (**a**) low and (**b**) high resolutions.

Thus, these results demonstrate the potential of a continuous dip-soaking process to fabricate an NP/IMC composite, as represented schematically in Figure 6 [12]. As envisioned, the production line consists of four different zones with a porous carrier going through. The membrane will not inhibit the impregnation process because it is much more permeable than the NP. An uncured NP/IMC composite can be fabricated with suitable roller speed control when the NP goes through the resin tank, after which excess surface resin is removed with a tip. The uncured composite then goes through the oven to be partially cured (usually 10%) to obtain enough strength but remain flexible enough, after which it finally gets packaged as NP/IMC nanotape (or prepreg). The nanotape product can be used to cover a polymer substrate to form a solid coating with additional heating to complete the cure, as discussed in the following section.

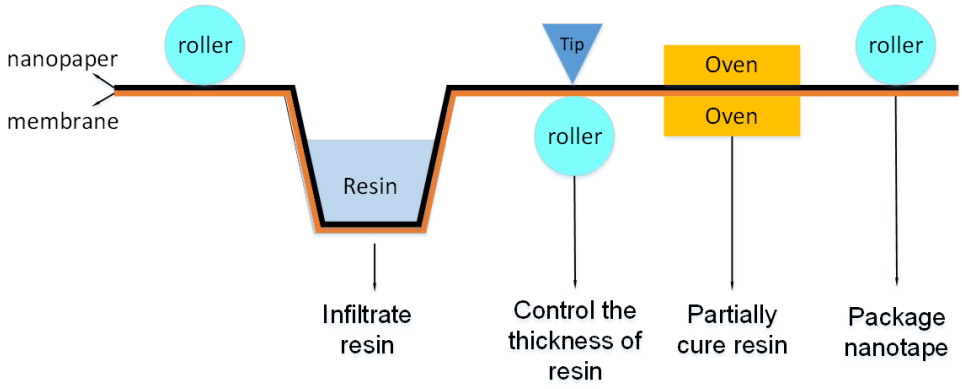

Figure 6. A continuous dip soaking process to fabricate nanocomposite.

3.2. Curing Analysis

As IMC resin is a heat-activated resin, the analyses of the curing stage were used to design the fabrication condition of the NP/IMC nanotape (or prepreg) and the curing of the prepreg as coatings. From the DSC curves shown in Figure 4, equations were developed for predicting the inhibition time and the reaction for times larger than the inhibition time, as shown in Equations (4) and (5), respectively, where T is in K.

In order to evaluate the technical viability of the fabrication process and the ability to predict curing during manufacturing, a nanotape was coated onto an SMC part. The effect of infiltration was negligible on the curing because the infiltration time (10 min) was much shorter than the inhibition time at an infiltration temperature of 50 °C. Thus, uncured the NP/IMC composite impregnated with the IMC resin was set up in an oven at 90 °C for 49 min (calculated utilizing the prediction equations) to prepare the prepreg, after which the prepreg was immediately coated onto an SMC part and cured at 150 °C for 6 h with a 1 kg part on top of a 2 cm by 2 cm prepreg. The results show that the prepreg could not be torn out of the SMC part, even with a knife, which demonstrates the good adhesion of the IMC resin to the SMC substrate as expected. Further experiments are ongoing to prototype the process.

$$t_z = e^{\left(\frac{12205}{T} - 25.67\right)} \tag{4}$$

$$\frac{d\alpha}{dt} = 3.81 \times 10^{10} e^{-\frac{10955}{T}} \alpha^{0.6238} \left(1 - e^{30.59 - 0.0884T} - \alpha\right)^{0.7131} \tag{5}$$

3.3. EMI Shielding Effectiveness

As the uncured NP/IMC composite or prepreg is stable at room temperature, it can be stacked to fabricate prepreg or coatings with different thicknesses, which increases its versatility for potential EMI shielding applications.

We used the same approach to prepare MWCNT NP and the EMI shielding testing method, as described in our previous work [11,12]. The NP itself (around 50 µm) had an effectiveness of 30 dB, while NP/epoxy, NP/PDMS, and NP/TPU composites all had an effectiveness of around 20 dB due to the swelling of the NP during the resin infiltration [9,10]. The EMI shielding effectiveness also showed a flat distribution within a frequency range of 13 MHz to 1.5 GHz [11,12].

To understand the shielding behavior of NP/IMC composite, six samples (samples 1 to 6) were prepared and tested using the same process for effectiveness tests. The approximate thickness of each layer was around 80 µm. The results suggest that the average NP/IMC composite effectiveness was 21 dB, as shown in Figure 7a. For the one-layer sample, our results indicate an enhanced effectiveness below 100 dB and a wave behavior of effectiveness (18.7 dB around 300 MHz and 19.1 dB around 900 MHz). Samples 1 to 6 were measurements of different nanopaper samples. The similarity of curves for these six samples additionally demonstrates the consistency of the fabrication process. By randomly

selecting and piling up samples, the EMI shielding effectiveness was analyzed for the NP/IMC composite with multiple layers, as shown in Figure 7b. The results suggest that the effectiveness of an NP/IMC composite increases with the increase in layers, while the partial increment decreases when the layers of the composite increase. For a six-layer sample, the average effectiveness reached 48 dB, while its effectiveness was over 65, 60, and 54 dB for a frequency below 100, 200, and 300 MHz, respectively. Also, for a frequency below 200 MHz, our result was even higher than the one-layer SWCNT NP (57 dB) described in our previous work [26]. The excellent EMI shielding effectiveness indicates the potential application at the very high frequency (VHF), especially for FM and TV broadcasts, cellular phones, and aviation communications, which are typically below 200 MHz.

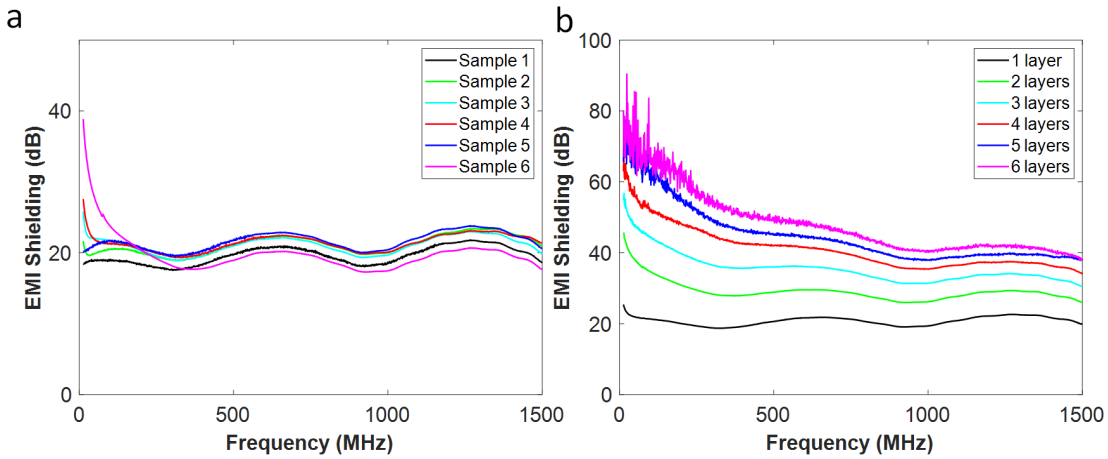

Figure 7. EMI shielding effectiveness for MWCNT NP/IMC composite (**a**) with one layer and (**b**) with multiple layers.

However, unlike NP/epoxy, NP/PDMS, or NP/TPU composites, the NP/IMC composite showed a wavy curve for the shielding effectiveness, which even became more significant for the multiple-layer samples. As the polymer inside the composite does not affect the absorption and reflection of waves [11,12], the wavy behavior of the effectiveness as a function of frequency should account for the transmission through multiple internal reflections [25].

4. Conclusions

In this study, we conducted an evaluation of the technical feasibility of fabricating an MWCNT NP/IMC composite. Additionally, we analyzed its curing behavior and electromagnetic interference (EMI) shielding effectiveness.

Our findings indicate that the infiltration temperature required for feasible NP/IMC composite fabrication ranges from 50 to 80 °C. To further investigate the infiltration of the nanopaper (NP), we performed thermogravimetric analysis (TGA) and scanning electron microscopy (SEM) tests, which confirmed the successful infiltration of the IMC resin into the MWCNT NP. Since the reaction temperature of the IMC resin was much larger than room temperature, it allowed for the proper design of the processing conditions for the infiltration and final curing of the coating using a curing model based on differential scanning calorimetry (DSC) data. This characteristic also allowed us to build multiple-layer NP/IMC composites by simply stacking one-layer composites.

Regarding the EMI shielding effectiveness, our results show that the one-layer NP/IMC composite exhibited an EMI shielding effectiveness of 21 dB. As we increased the number of layers to six, the average effectiveness reached 48 dB. For frequencies below 100, 200, and 300 MHz, it exceeded 65, 60, and 54 dB, respectively, which indicates the potential use for high-frequency applications.

As the next step, we plan to build a prototype to demonstrate the entire fabrication process and validate its industrial viability.

Author Contributions: Conceptualization, methodology, writing—review and editing: K.C., D.Z. and J.M.C.; supervision, project administration, funding acquisition: J.M.C.; Others: K.C. and J.M.C. All authors have read and agreed to the published version of the manuscript.

Funding: The financial support of Synthomer is greatly appreciated. We also thank Jiangsu Funding Program for Excellent Postdoctoral Talent.

Data Availability Statement: The data presented in this study are available on request from the corresponding author. The data are not publicly available due to our policy for developing new products.

Conflicts of Interest: The authors declare no conflict of interest.

References

1. De Volder, M.F.L.; Tawfick, S.H.; Baughman, R.H.; Hart, A.J. Carbon nanotubes: Present and future commercial applications. *Science* **2013**, *339*, 535–539. [CrossRef] [PubMed]
2. Geetha, S.; Kumar, K.K.S.; Rao, C.R.K.; Vijayan, M.; Trivedi, D.C.K. EMI shielding: Methods and materials—A review. *J. Appl. Polym. Sci.* **2009**, *112*, 2073–2086. [CrossRef]
3. Yavuz, Ö.; Manoj, K.R.; Aldissi, M. Electromagnetic applications of conducting and nanocomposite materials. In *The New Frontiers of Organic and Composite Nanotechnology*; Elsevier: Amsterdam, The Netherlands, 2008; pp. 435–475.
4. Henz, D. Shielding chips reduce effects on eeg brain activity induced by electromagnetic radiation in the 5G range. *Psychophysiology* **2021**, *58*, s58.
5. Bertašius, P.; Plyushch, A.; Macutkevič, J.; Banys, J.; Selskis, A.; Platnieks, O.; Gaidukovs, S. Multilayered Composites with Carbon Nanotubes for Electromagnetic Shielding Application. *Polymers* **2023**, *15*, 1053. [CrossRef] [PubMed]
6. Kim, M.; Kim, H.; Byun, S.; Jeong, S.; Hong, Y.; Joo, J.; Song, K.; Kim, J.; Lee, C.; Lee, J. PET fabric/polypyrrole composite with high electrical conductivity for EMI shielding. *Synth. Met.* **2002**, *126*, 233–239. [CrossRef]
7. Jalali, A.; Zhang, R.; Rahmati, R.; Nofar, M.; Sain, M.; Park, C.B. Recent progress and perspective in additive manufacturing of EMI shielding functional polymer nanocomposites. *Nano Res.* **2022**, *16*, 1–17. [CrossRef]
8. Lee, Y.H.; Wang, L.Y.; Tsai, C.Y.; Lee, C.W. Self-healing nanocomposites with carbon nanotube/graphene/Fe3O4 nanoparticle tricontinuos networks for electromagnetic radiation shielding. *ACS Appl. Nanomater.* **2022**, *5*, 16423–16439. [CrossRef]
9. Chen, W.; Wang, J.; Zhang, B.; Wu, Q.; Su, X. Enhanced electromagnetic interference shielding properties of carbon fiber veil/Fe_3O_4nanoparticles/epoxy multiscale composites. *Mater. Res. Express* **2017**, *4*, 126303. [CrossRef]
10. Bertasius, P.; Macutkevic, J.; Banys, J.; Gaidukovs, S.; Barkane, A.; Vaivodiss, R. Synergy effects in dielectric and thermal properties of layered ethylene vinyl acetate composites with carbon and Fe_3O_4 nanoparticles. *J. Appl. Polym. Sci.* **2019**, *137*, 48814. [CrossRef]
11. Zhang, D.; Yang, H.; Pan, J.; Lewis, B.; Zhou, W.; Cai, K.; Benatar, A.; Lee, L.J.; Castro, J.M. Multi-functional CNT nanopaper polyurethane nanocomposite fabricated by ultrasonic infiltration and dip soaking processes. *Compos. Part B Eng.* **2019**, *182*, 107646. [CrossRef]
12. Zhang, D.; Cai, K.; Pan, J.; Lee, L.J.; Castro, J.M. A novel carbon nanotube nanopaper polyurethane coating for fiber reinforced composite substrates. *Polym. Eng. Sci.* **2020**, *61*, 1041–1049. [CrossRef]
13. Bauhofer, W.; Kovacs, J.Z. A review and analysis of electrical percolation in carbon nanotube polymer composites. *Compos. Sci. Technol.* **2009**, *69*, 1486–1498. [CrossRef]
14. Al-Saleh, M.H.; Sundararaj, U. A review of vapor grown carbon nanofiber/polymer conductive composites. *Carbon* **2009**, *47*, 2–22. [CrossRef]
15. Al-Saleh, M.H.; Saadeh, W.H.; Sundararaj, U. EMI shielding effectiveness of carbon based nanostructured polymeric materials: A comparative study. *Carbon* **2013**, *60*, 146–156. [CrossRef]
16. Bertasius, P.; Meisak, D.; Macutkevic, J.; Kuzhir, P.; Selskis, A.; Volnyanko, E.; Banys, J. Fine Tuning of Electrical Transport and Dielectric Properties of Epoxy/Carbon Nanotubes Composites via Magnesium Oxide Additives. *Polymers* **2019**, *11*, 2044. [CrossRef]
17. Wang, Y.; Zhou, P.; Luo, S.; Guo, S.; Shao, Q.; Guo, X.; Liu, Z.; Shen, J.; Wang, B.; Guo, Z. In situ polymerized poly (acrylic acid)/alumina nanocomposites for Pb^{2+} adsorption. *Adv. Polym. Technol.* **2018**, *37*, 2981–2996. [CrossRef]
18. Hu, Z.; Zhang, D.; Lu, F.; Yuan, W.; Xu, X.; Zhang, Q.; Liu, H.; Shao, Q.; Guo, Z.; Huang, Y. Multistimuli-Responsive Intrinsic Self-Healing Epoxy Resin Constructed by Host–Guest Interactions. *Macromolecules* **2018**, *51*, 5294–5303. [CrossRef]
19. Chapartegui, M.; Barcena, J.; Irastorza, X.; Elizetxea, C.; Fernandez, M.; Santamaria, A. Analysis of the conditions to manufacture a MWCNT buckypaper/benzoxazine nanocomposite. *Compos. Sci. Technol.* **2012**, *72*, 489–497. [CrossRef]
20. Ashrafi, B.; Guan, J.; Mirjalili, V.; Hubert, P.; Simard, B.; Johnston, A. Correlation between Young's modulus and impregnation quality of epoxy-impregnated SWCNT buckypaper. *Compos. Part A* **2010**, *41*, 1184–1191. [CrossRef]
21. Kaiyu, C. Developing New In-Mold Coating Formulations for Electrostatic Painting and Nano-Tapes for Electromagnetic Interference Shielding. Ph.D. Thesis, The Ohio State University, Columbus, OH, USA, 2021.
22. Ko, S. Selecting Best Compromises among Performance Measures during In-Mold Coating of Sheet Molding Compound Compression Molding Parts. Ph.D. Thesis, The Ohio State University, Columbus, OH, USA, 2015.

23. Kenny, J.M. Determination of autocatalytic kinetic model parameters describing thermoset cure. *J. Appl. Polym. Sci.* **1994**, *51*, 761–764. [CrossRef]
24. Bhuyan, M.S.K. Further Applications of Reactive In-Mold Coating (IMC): Effect of Inhibitor and Carbon Nanoparticles. Ph.D. Dissertation, The Ohio State University, Columbus, OH, USA, 2018.
25. Patle, V.; Kumar, R.; Sharma, A.; Dwivedi, N.; Muchhala, D.; Chaudhary, A.; Mehta, Y.; Mondal, D.; Srivastava, A. Three dimension phenolic resin derived carbon-CNTs hybrid foam for fire retardant and effective electromagnetic interference shielding. *Compos. Part C* **2020**, *2*, 100020. [CrossRef]
26. Zhao, Y.; Cabrera, E.D.; Zhang, D.; Sun, J.; Kuang, T.; Yang, W.; Lertola, M.J.; Benatar, A.; Castro, J.M.; Lee, L.J. Ultrasonic processing of MWCNT nanopaper reinforced polymeric nanocomposites. *Polymer* **2018**, *156*, 85–94. [CrossRef]